LAWRENCE
LIVERMORE
NATIONAL
LABORATORY

LLNL-JRNL-511215

An Analytic Treatment of Source Photon Emission Times to Reduce Noise in Implicit Monte Carlo Calculations

T. J. Trahan, N. A. Gentile

November 7, 2011

Transport Theory and Statistical Physics

ANALYTIC TREATMENT OF SOURCE PHOTON EMISSION TIMES TO REDUCE NOISE IN IMPLICIT MONTE CARLO CALCULATIONS

Travis J. Trahan[1] **and Nicholas A. Gentile**[2]

[1] Department of Nuclear Engineering and Radiological Sciences
University of Michigan
2355 Bonisteel Blvd., Ann Arbor, MI, 48109
tjtrahan@umich.edu

[2] Lawrence Livermore National Laboratory
P.O. Box 808, Livermore, CA 94551
gentile1@llnl.gov

ABSTRACT

Statistical uncertainty is inherent to any Monte Carlo simulation of radiation transport problems. In space-angle-frequency independent radiative transfer calculations, the uncertainty in the solution is entirely due to random sampling of source photon emission times. We have developed a modification to the Implicit Monte Carlo algorithm that eliminates noise due to sampling of the emission time of source photons. In problems that are independent of space, angle, and energy, the new algorithm generates a smooth solution, while a standard implicit Monte Carlo solution is noisy. For space and angle dependent problems, the new algorithm exhibits reduced noise relative to standard implicit Monte Carlo in some cases, and comparable noise in all other cases. The improvements are limited to short time scales; over long time scales, noise due to random sampling of spatial and angular variables tends to dominate the noise reduction from the new algorithm.

Key Words: radiation transport, implicit Monte Carlo, noise reduction

1. Introduction

In this paper, we present a modification to the Implicit Monte Carlo (IMC) algorithm to reduce statistical noise in radiation transport calculations. We consider problems of radiative transfer, which is the process by which photons are emitted by hot matter, transported, and ultimately reabsorbed. These problems require the solution of two coupled equations for radiation intensity, $I(\boldsymbol{x}, \boldsymbol{\Omega}, t)$, and matter energy density, $\epsilon(\boldsymbol{x}, t)$ (Pomraning, 2005):

$$\frac{1}{c}\frac{\partial I}{\partial t}+\boldsymbol{\Omega}\cdot\nabla I = -(\sigma_s(\boldsymbol{x},t)+\sigma_a(\boldsymbol{x},t))I+\frac{1}{4\pi}c\sigma_p(\boldsymbol{x},t)aT^4b(T)+\int_{4\pi}\sigma_s(\boldsymbol{x},t)I(\boldsymbol{x},\boldsymbol{\Omega}',t)\mathrm{d}\Omega'+S_I(\boldsymbol{x},\boldsymbol{\Omega},t)\,, \tag{1a}$$

$$\frac{\partial \epsilon}{\partial t} = \int_{4\pi}\sigma_a(\boldsymbol{x},t)I(\boldsymbol{x},\boldsymbol{\Omega}',t)\mathrm{d}\Omega' - c\sigma_p aT^4 + S_\epsilon(\boldsymbol{x},t)\,, \tag{1b}$$

where $\sigma_a(\boldsymbol{x}, t)$ = absorption opacity, $\sigma_s(\boldsymbol{x}, t)$ = scattering opacity, $\sigma_p(\boldsymbol{x}, t)$ = Planck mean opacity, $b(T)$ = normalized Planck function, $S_I(\boldsymbol{x}, \boldsymbol{\Omega}, t)$ = photon sources, $S_\epsilon(\boldsymbol{x}, t)$ = thermal sources.

Equations (1a) and (1b) are written in a frequency independent, isotropic scattering form for simplicity. Frequency dependence and anisotropic scattering do not affect the derivation of our method.

Equations (1a) and (1b) are coupled equations. Photons are absorbed by matter, thereby increasing its temperature. The hot matter emits photons, which then decreases its temperature. The T^4 coupling term makes thes equations stiff, and so an explicit time stepping algorithm often yields an oscillatory solution. Instead, we solve these equations using the Implicit Monte Carlo method, which has improved stability properties (Fleck and Cummings, 1971). The details of this method are not discussed here.

In this paper, we will focus only on the way in which source photons are emitted. Source photons, whether they are from arbitrary sources, $S_I(\boldsymbol{x}, \boldsymbol{\Omega}, t)$, or from thermal emission from the hot matter, $\frac{1}{4\pi} c\sigma_p(\boldsymbol{x}, t) a T^4 b(T)$, are assumed to be uniformly emitted within a given time step. We begin in Section 2 by showing that the uniform random sampling of the source photon emission times introduces noise into IMC calculations, even for problems that are independent of space, angle, and frequency.

It has previously been shown that the source photon emission times can be treated analytically, thereby eliminating the need to randomly sample the emission times (Gentile and Trahan, 2011). This method completely eliminates noise due to emission time sampling. We will rederive this method in Section 3.

We then explore the effectiveness of the new algorithm through a series of test problems in Section 4. We conclude with a brief discussion in Section 5.

2. Noise Due to Emission Time Sampling in Space, Angle, and Frequency Independent Problems

We will first show that noise exists in the IMC solution even in problems that are independent of space, angle, and frequency. In this case, noise is entirely a result of randomly sampling source photon emission times.

Let us examine the case of an infinite medium problem with gray, constant opacities, and with matter and radiation at equilibrium at temperature T, simulated with the IMC method. The census photons in a volume V representing the initial radiation all initially have time $t = 0$ and have a total energy

$$E_c(t = 0) = aT^4 V\,. \tag{2}$$

During a time step of size Δt, the energy of each census photon will decrease by a factor $\exp[-\sigma c \Delta t]$. The total energy in census photons at the end of the time step will therefore be

$$E_c(t = \Delta t) = aT^4 V \exp[-\sigma c \Delta t]\,. \tag{3}$$

To simulate thermal emission, we will make N_s thermal source photons, each with a different, randomly sampled initial time, $t_{i,p} \in [0, t]$. We will assume all N_s photons have the same initial energy

$$E_p(t = 0) = ac\sigma T^4 V \Delta t / N_s\,. \tag{4}$$

Since $t_{i,p}$ is unique for each photon, they will all reach time Δt with different energies:

$$E_p(t = \Delta t) = (ac\sigma T^4 V \Delta t / N_s)\exp[-\sigma c(\Delta t - t_{i,p})]\,. \tag{5}$$

The sum of these energies will be

$$E_t(t = \Delta t) \equiv \sum_{p=1}^{N_s} E_p(t = \Delta t) = ac\sigma T^4 V \Delta t \frac{1}{N_s} \sum_{p=1}^{N_s} \exp[-\sigma c(\Delta t - t_{i,p})]\,. \tag{6}$$

If we let $N_s \to \infty$, we see that this sum is a Monte Carlo estimate for an integral over all posible emission times:

$$\begin{aligned} E_t(t = \Delta t) &= \lim_{N_s \to \infty} ac\sigma T^4 V \Delta t \frac{1}{N_s} \sum_{p=1}^{N_s} \exp[-\sigma c(\Delta t - t_{i,p})]\,, \\ &= ac\sigma T^4 V \Delta t \frac{1}{\Delta t} \int_0^{\Delta t} \exp[-\sigma c(\Delta t - \tau)]\mathrm{d}\tau\,. \end{aligned} \tag{7}$$

By performing the integral in Eq. (7) we find that, in the limit of large N_s, the total radiation energy due to thermally emitted photons at $t = \Delta t$ will be

$$E_t(t = \Delta t) = aT^4 V \left(1 - \exp[-\sigma c \Delta t]\right)\,. \tag{8}$$

Adding Eqs. (3) and (8) yields:

$$E_c(t = \Delta t) + E_t(t = \Delta t) = aT^4 V\,,$$

which is exactly the value necessary to maintain thermal equilibrium. The matter energy will also be the same as the initial value, by energy conservation. With a finite number of photons, we will not maintain thermal equilibrium exactly, because the sum in Eq. (6) will only approximate the integral in Eq. (7), with an error that is proportional to $N_s^{-1/2}$ (Kalos and Whitlock, 2008). Furthermore, the noise will grow as Δt increases because the integrand in Eq. (7) will vary more within the limits of integration, and so the integral is more poorly approximated by the sum in Eq. (6).

This behavior can be observed in Figs. 1 and 2. These plots show the matter and radiation temperatures, T_m and T_r respectively, as a function of time according to an IMC simulation. The simulation is of a one-zone cube with unit length in each direction. All faces have reflecting boundaries, making it effectively an infinite medium problem. The material temperature is initialized to $T_{m,0} = 1.0$ in Fig. 1, and to 1.1 and 0.5 in Fig. 2. The radiation temperature is initialized such that the equilibrium temperature is 1.0. The material has heat capacity $c_v = 1.0$, and an absorption opacity $\sigma = 10$. The unit system is defined such that $a = c = 1.0$. The simulation used 100 photons per time step. In the equilibrium case, Fig. 1, varying time steps are used, with $\Delta t = 0.001$ for $t \in [0, 1]$, $\Delta t = 0.01$ for $t \in (1, 2]$, and $\Delta t = 0.1$ for $t \in (2, 3]$.

In Fig. 1, we see that noise does indeed increase as the time step size, Δt, increases. In Fig. 2, we see that statistical noise from emission time sampling is greater when the matter temperature is large relative the radiation temperature. Note that the radiation temperature is initially smooth in Fig. 2(b) when the matter is initially cold, while it is always noisy in Fig. 2(a) because the

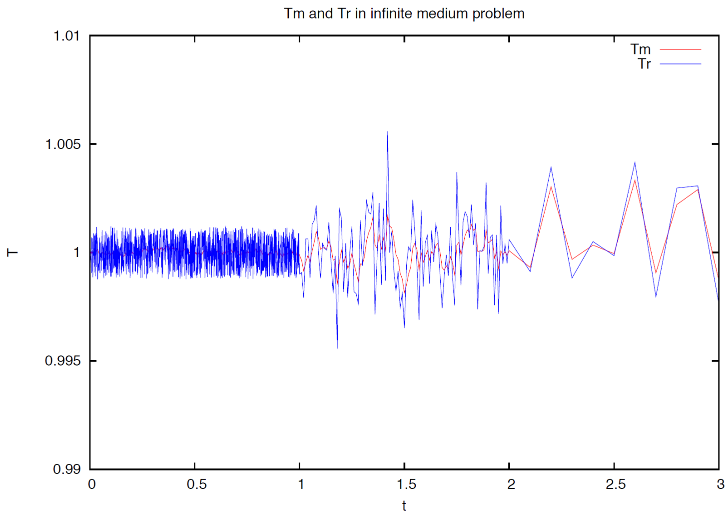

Figure 1: T_m and T_r in a grey, infinite medium problem in thermal equilibrium at $T = 1.0$ simulated by IMC. $\Delta t = 0.001$ for $t \in [0, 1]$, $\Delta t = 0.01$ for $t \in (1, 2]$, and $\Delta t = 0.1$ for $t \in (2, 3]$.

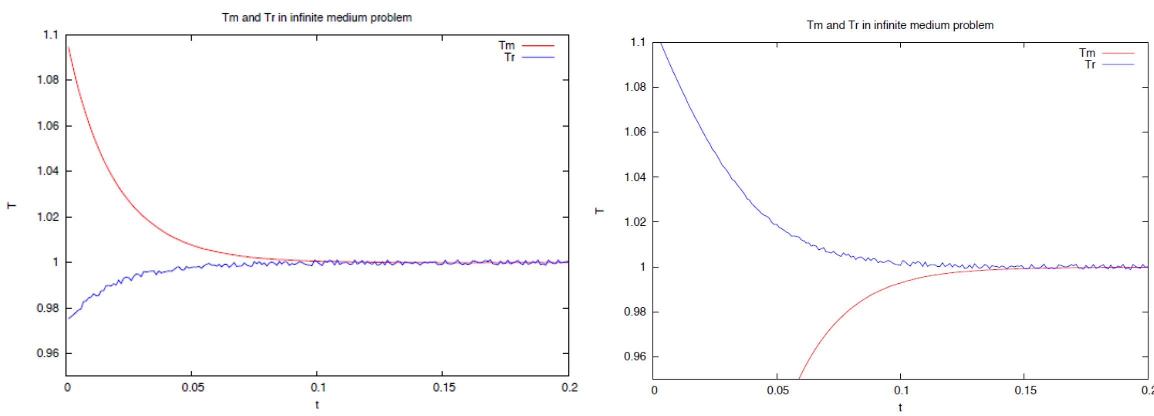

(a) $T_{m,0} = 1.1$

(b) $T_{m,0} = 0.5$

Figure 2: T_m and T_r in a grey, infinite medium problem simulated by IMC. $T_{r,0}$ is chosen such that the equilibrium temperature is 1.0

matter is always hot. This behavior occurs because census photon times are deterministic (all census photons begin at the start of the time step), and hence there is no noise in the census photon radiation energy in the infinite medium case. When the radiation temperature is large relative to the matter temperature, most of the energy is carried by census photons, and so the noise in the source photon radiation energy is small.

3. Modified Source Treatment to Eliminate Noise Due to Emission Time Sampling

In this section, we will show how the random sampling of source photon emission times can be eliminated from the IMC algorithm. In IMC, the physical properties of the system are assumed to be constant within a time step. As a result, photon behavior and energy deposition is independent of when it occurs within a time step.

Therefore, for each photon path, we can consider what would have happened if the photon had been born at time $\tau \in [t^n, t^{n+1}]$. Then we can analytically calculate how much energy would have been absorbed on this path, E_a, how much radiation energy this photon would have represented, E_r, and determine whether or not the photon would have reached census and with what energy, E_c. Then we will calculate the average for all possible emission times $\tau \in [t^n, t^{n+1}]$. We refer to our new algorithm as "smooth emission IMC" because we smooth the emission time of the source photons over the entire time step. We refer to the modified source photons as "smooth source photons".

As in IMC, we sample a position, direction, frequency, and energy E_p for each source photon, and the energy will decrease exponentially along each photon path: $E_p(s) = E_p(s_0)\exp[-\sigma(s - s_0)]$. However, we do not sample an emission time. Instead of the source photon having a time, it will have a distance traveled, s_p, with an initial value of 0. The source photon will travel a total distance $c\Delta t$ in the time step, unless it exits the problem through a boundary. After traveling a distance s, physical source photons born in $[t^{n+1} - s/c, t^{n+1}]$ have already reached census. Therefore, the radiation energy represented by the smooth source photon after it has moved a distance s must be attenuated by absorption *and* by the fact that a fraction of the physical source photons are reaching census. The additional attenuation factor is:

$$\frac{\Delta t - s/c}{\Delta t - s_0/c} = \text{fraction of photons that have not reached census at } s_0 \text{ that do reach census by } s. \tag{9}$$

The energy of the source photon will be either absorbed, leave the problem through a boundary, or reach census as the photon reaches $s_p = c\Delta t$.

First, we calculate the average radiation energy of the smooth photons. The radiation energy of the smooth photon at the end of a path from s_0 to s is:

$$E_{r,smooth}(s) = E_p(s_0)\exp[-\sigma(s - s_0)]\frac{\Delta t - s/c}{\Delta t - s_0/c}\,. \tag{10}$$

Then the average radiation energy over the photon path is:

$$\begin{aligned}
\langle E_r \rangle_{s_0,s_1} &= \frac{\int_{s_0}^{s_1} E_{r,smooth}(s)\mathrm{d}s}{\int_{s_0}^{s_1}\mathrm{d}s} = \frac{\int_{s_0}^{s_1} E_p(s_0)\exp[-\sigma(s - s_0)]\frac{\Delta t - s/c}{\Delta t - s_0/c}\mathrm{d}s}{s_1 - s_0}\,,\\
&= \frac{E_p(s_0)}{\sigma\,(s_1 - s_0)\,(\Delta t - s_0/c)}\\
&\qquad \times \left[\Delta t\,(1 - \exp[-\sigma(s_1 - s_0)]) - \frac{1}{c\sigma}\,(\exp[-\sigma(s_1 - s_0)]\,(1 + s_1\sigma) - (1 + s_0\sigma))\right]\,,\\
&= \text{average energy of the photon on the path from } s_0 \text{ to } s_1.
\end{aligned} \tag{11}$$

Then the average radiation energy of the smooth photon during the time step is the sum of the averages on each path weighted by the fractional path length:

$$E_r = \sum_{p=1}^{N_{paths}} \langle E_r \rangle_{s_0,s_1} \frac{s_1 - s_0}{c\Delta t} \,. \tag{12}$$

Next, we calculate the energy reaching census on each path. We see that:

$$\frac{\mathrm{d}s/c}{\Delta t} = \text{fraction of all photons that reach census after traveling a distance } s' \in [s, s+\mathrm{d}s],$$

$$\frac{\Delta t - s_0/c}{\Delta t} = \text{fraction of photons that have not reached census at } s_0,$$

and so:

$$\begin{aligned}\left(\frac{\mathrm{d}s/c}{\Delta t}\right) / \left(\frac{\Delta t - s_0/c}{\Delta t}\right) &= \frac{\mathrm{d}s/c}{\Delta t - s_0/c}\,, \\ &= \text{fraction of photons that have not reached census at } s_0 \text{ that do} \\ &\quad\ \text{reach census after traveling a distance } s' > s_0,\ s' \in [s, s+\mathrm{d}s].\end{aligned}$$

The energy of a physical source photon after traveling from s_0 to s is:

$$E_{r,physical}(s) = E_p(s_0)\exp[-\sigma(s - s_0)] \,.$$

Thus, the total energy reaching census on a path from s_0 to s_1 is:

$$\begin{aligned}E_c(s_0, s_1) &= \int_{s_0}^{s_1} \frac{E_p(s_0)}{c(\Delta t - s_0/c)} \exp[-\sigma(s - s_0)]\mathrm{d}s'\,, \\ &= \frac{E_p(s_0)}{c\sigma(\Delta t - s_0/c)} \left[1 - \exp[-\sigma(s_1 - s_0)]\right] \,.\end{aligned} \tag{13}$$

Finally, we calculate the total energy absorbed along the path from s_0 to s_1. This is done by simple energy conservation, which demands that:

$$E_a(s_0, s_1) + E_c(s_0, s_1) + E_{r,smooth}(s_1) = E_{r,smooth}(s_0) \,. \tag{14}$$

Introducing Eq. (10) into Eq. (14) and rearranging yields:

$$E_a(s_0, s_1) = E_{r,smooth}(s_0) \left[1 - \exp[-\sigma(s_1 - s_0)] \frac{\Delta t - s_1/c}{\Delta t - s_0/c}\right] - E_c(s_0, s_1) \,. \tag{15}$$

Equations (11), (13), and (15) define the radiation energy, energy reaching census, and absorbed energy along each photon path from s_0 to s_1. We sample all other variables and track the photon through the zones as we do in standard IMC. Census photons are treated exactly as in standard IMC; only source photons are treated differently, and only until the end of the time step in which they are born.

One complication that arises from this algorithm is that now each photon path contributes energy to census. Source photons no longer reach the end of the time step, at least in the usual sense, and so we have no source photons to serve as census photons for the next time step. We must select source photons at random to carry the energy during the next time step. To do this, we sample an emission time for each photon, but use it only to determine when to save the state of the photon to a list. Source photons are still transported after they have been saved until they have traveled a distance $c\Delta t$, they are destroyed, or they leak out of the system. After all source photons have been transported in this manner, we distribute the total census energy, E_c, among the saved photons in proportion to their energies at the time they were saved.

We now apply the smooth emission algorithm to the same problems described in Section II. In Figs. 3 and 4, we see that the new algorithm yields a smooth solution for equilibrium and non-equilibrium cases.

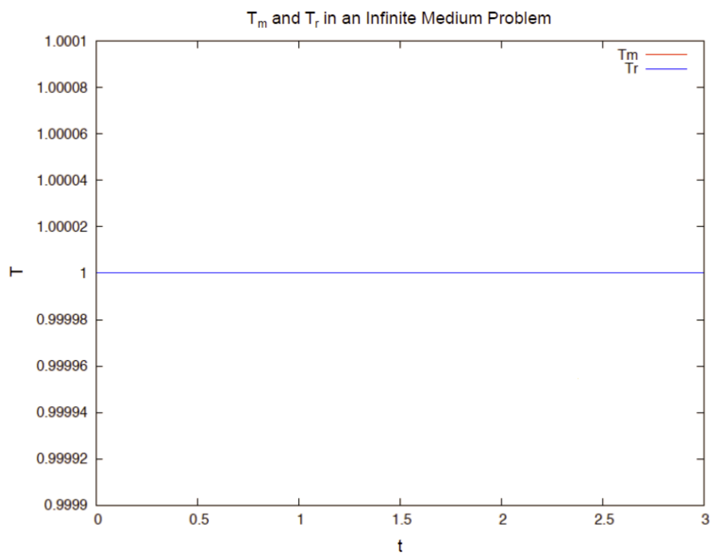

Figure 3: T_m and T_r in a grey, infinite medium problem in thermal equilibrium at $T = 1.0$ simulated by smooth emission IMC. $\Delta t = 0.001$ for $t \in [0,1]$, $\Delta t = 0.01$ for $t \in (1,2]$, and $\Delta t = 0.1$ for $t \in (2,3]$.

4. Numerical Results for Space and Angle Dependent Problems

We will now demonstrate the effectiveness of the smooth emission IMC algorithm on problems with space and angle dependence. Spatial and angular variables are also randomly sampled in the IMC algorithm. As a result, the equilibrium solution in problems with multiple spatial zones will be noisy due to particles randomly crossing zone boundaries, even with the new algorithm. We expect that for problems in which the dominant source of noise is the sampling of the emission time, the smooth emission IMC algorithm will reduce noise in the solution relative to standard IMC.

Noise due to sampling the spatial and angular variables only shows up as photons cross zone boundaries. Therfore, for simulations in which most source photons remain in the zone they were created in, emission time sampling should be more important than the sampling of other

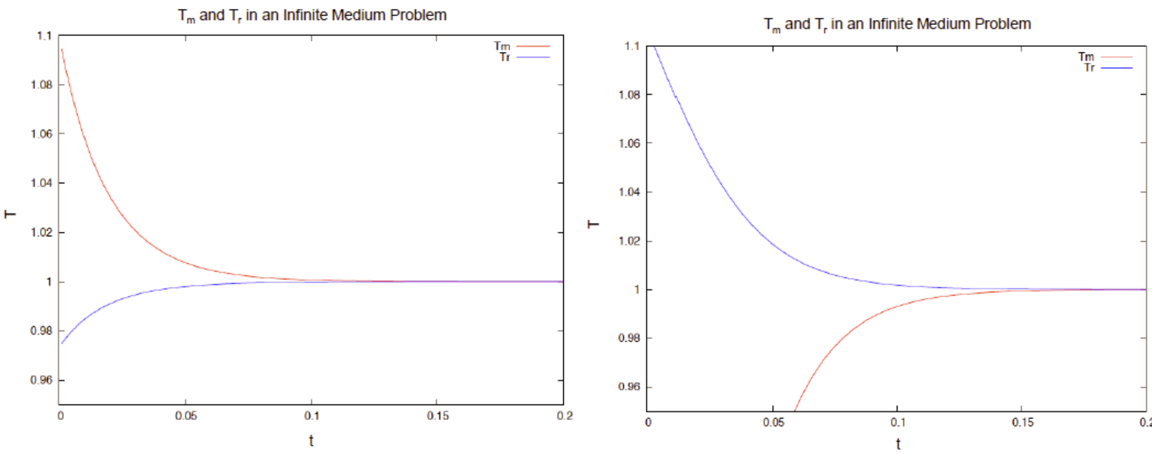

(a) $T_{m,0} = 1.1$ (b) $T_{m,0} = 0.5$

Figure 4: T_m and T_r in a grey, infinite medium problem simulated by smooth emission IMC. $T_{r,0}$ is chosen such that the equilibrium temperature is 1.0

variables. The new algorithm should reduce noise for such simulations. This condition is met if the mean free path of photons is small compared to the size of the zone, because few photons will stream from one zone to another:

$$\frac{1}{\sigma} \ll \Delta x, \text{ or } \frac{1}{\sigma \Delta x} \ll 1 \,. \tag{16}$$

This condition is also met if the time step size is sufficiently small that source photons do not migrate far from their point of emission relative to the size of the zone. We define:

$$c\Delta t\sigma \equiv N \propto \text{the average number of photon paths per time step.}$$

Assuming that the photon paths are not correlated in direction, the average distance traveled by a photon on N paths from the point of emission will be:

$$\sqrt{N}\frac{1}{\sigma} = \sqrt{\frac{c\Delta t}{\sigma}} \,.$$

This leads to the desired condition:

$$\sqrt{\frac{c\Delta t}{\sigma}} \ll \Delta x, \text{ or } \sqrt{\frac{c\Delta t}{\sigma}}/\Delta x \ll 1 \,. \tag{17}$$

We have already seen that the noise due to emission time sampling is greater when a significant portion of the energy is carried by source photons rather than census photons (Fig. 2). This occurs when:

$$\frac{E_{emitted}}{E_{census}} = \frac{fc\sigma aT^4V\Delta t}{aT^4V} = fc\sigma\Delta t \gg 1 \,. \tag{18}$$

When Eq. (18) holds, the smooth emission algorithm should be more effective. Here, f is the Fleck factor that arises in the IMC algorithm (Fleck and Cummings, 1971).

Thus, if a particular simulation satisfies Eqs. (16), (17), and (18), the smooth emission IMC algorithm should reduce noise in the solution. To demonstrate, we study a one-dimensional, homogenous problem with transmitting boundaries. Face sources with $T = 1.0$ at each end hold the problem in thermal equilbrium. The system is divided into 10 spatial zones, and the total domain size is determined by the desired mesh size, Δx. All tests are run to 1000 time steps with 10000 particles per step. Units are chosen such that $a = c = 1.0$. The smooth emission algorithm and standard IMC algorithm are applied to several simulations with different values of Δt, Δx, and heat capacity, c_v. The two algorithms are compared qualitatively by visual inspection of the noise in the equilibrium solution.

Figure 5 shows an example of a simulation for which the smooth emission algorithm outperforms standard IMC. For this simulation, $1/(\sigma\Delta x) = 0.001$, $\sqrt{c\Delta t/\sigma}/\Delta x = 0.0003162$, and $E_{emitted}/E_{census} = 0.07143$. Therefore, by Eqs. (16), (17), and (18), we expect significant noise reduction when using the smooth emission algorithm, which is exactly what is observed. Looking at Fig. 5, we see that in zone 1, which is a boundary zone, the temperature rises uniformly as the boundary source heats the problem. The uniformity is only disturbed as particles enter or exit this zone. In zone 2, which is an interior zone, the temperature does not change at all unless a particle enters or exits this zone.

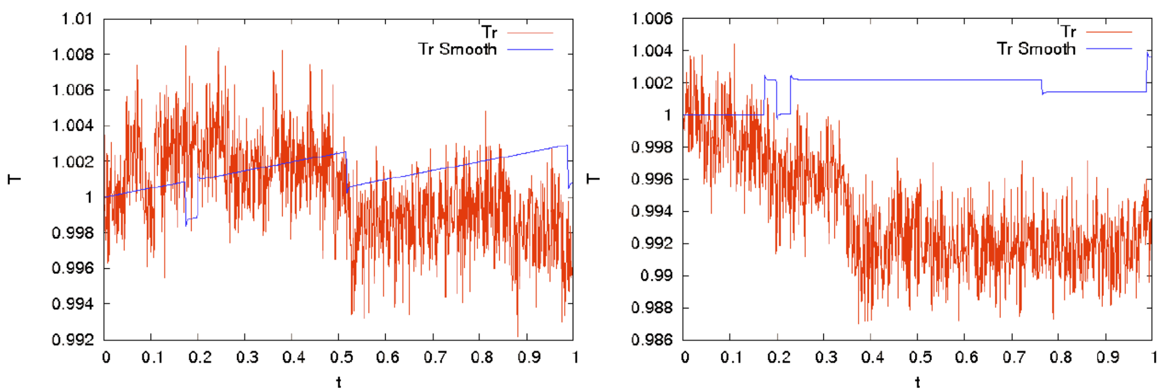

(a) Zone 1

(b) Zone 2

Figure 5: Radiation temperature in an equilibrium problem simulated by standard IMC (T_r) and by smooth emission IMC (T_r Smooth). $\Delta t = 0.001$, $\Delta x = 10.0$, and $c_v = 1.0$. Therefore, $1/(\sigma\Delta x) = 0.001$, $\sqrt{c\Delta t/\sigma}/\Delta x = 0.0003162$, and $E_{emitted}/E_{census} = 0.07143$.

Figure 6 shows an example of a simulation for which the smooth emission algorithm does not outperform standard IMC. For this simulation, $1/(\sigma\Delta x) = 1.0$, $\sqrt{c\Delta t/\sigma}/\Delta x = 5.0$, and $E_{emitted}/E_{census} = 0.2475$. These values do not satisfy Eqs. (16), (17), and (18), and so the poor performance is expected. While it is still true that the temperature in a zone cannot change unless photons cross zone boundaries, photons cross zone boundaries in every time step for this simulation, so the noise is not reduced.

Table I summarizes the performance of the smooth emission IMC algorithm for a series of runs with $c_v = 1.0$. From Table I it is clear that smooth emission IMC becomes more effective as $1/(\sigma\Delta x)$ and $\sqrt{c\Delta t/\sigma}/\Delta x$ get smaller, as expected.

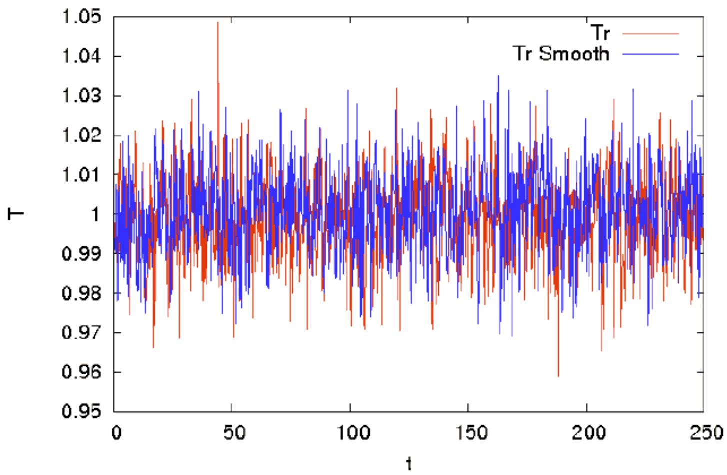

Figure 6: Radiation temperature in an equilibrium problem simulated by standard IMC (T_r) and by smooth emission IMC (T_r Smooth). $\Delta t = 0.25$, $\Delta x = 0.01$, and $c_v = 1.0$. Therefore, $1/(\sigma\Delta x) = 1.0$, $\sqrt{c\Delta t/\sigma}/\Delta x = 5.0$, and $E_{emitted}/E_{census} = 0.2475$.

Table I. Qualitative performance of the smooth emission algorithm vs. standard IMC with $c_v = 1.0$. Sig. = significant, Lim. = limited. $E_e = E_{emitted}$, $E_c = E_{census}$.

	Run 1	Run 2	Run 3	Run 4	Run 5	Run 6	Run 7	Run 8	Run 9	Run 10	Run 11	Run 12
c_v	1	1	1	1	1	1	1	1	1	1	1	1
σ	100	100	100	100	100	100	100	100	100	100	100	100
Δt	0.001	0.01	0.25	0.001	0.01	0.25	0.001	0.01	0.25	0.001	0.01	0.25
Δx	10	10	10	1	1	1	0.1	0.1	0.1	0.01	0.01	0.01
1/($\sigma\Delta$x)	0.001	0.001	0.001	0.01	0.01	0.01	0.1	0.1	0.1	1	1	1
sqrt(cΔt/σ)/Δx	3E-04	0.001	0.005	0.003	0.01	0.05	0.032	0.1	0.5	0.316	1	5
E_e/E_c	0.071	0.2	0.248	0.071	0.2	0.248	0.071	0.2	0.248	0.071	0.2	0.248
Improvement	Best	Sig.	Sig.	Sig.	Sig.	Lim.	Lim.	Lim.	None	None	None	None

Table II summarizes the performance of the smooth emission IMC algorithm for the same series of test problems, except with $c_v = 4000$. The only effect of increasing c_v is to increase $E_{emitted}/E_{census}$, which should improve the performance of the new algorithm. Table II indicates that this is indeed the case. We see that more test problems show significant improvement and fewer show no improvement. Furthermore, in some cases, problems with larger values of $1/(\sigma\Delta x)$ and $\sqrt{c\Delta t/\sigma}/\Delta x$ are more affected than similar problems with smaller values of $1/(\sigma\Delta x)$ and $\sqrt{c\Delta t/\sigma}/\Delta x$ due to the increased amount of energy carried by source photons.

Now we will apply the smooth emission algorithm to more realistic problems. First, we consider a Marshak wave test problem in a homogeneous medium with transmitting boundaries. A face source with $T = 1.0$ keV heats the problem from the left side. The medium is initially cold and in thermal equilibrium, with $T_r = T_m = 0.003162$ keV. There are twenty zones with $\Delta x = 0.1$ cm. The simulation is run to a time $t_{max} = 5 \times 10^{-7}$ s with a time step of $\Delta t = 10^{-12}$ s. There

Table II. Qualitative performance of the smooth emission algorithm vs. standard IMC with $c_v = 4000$.. Sig. = significant, Lim. = limited. $E_e = E_{emitted}$, $E_c = E_{census}$.

	Run 1	Run 2	Run 3	Run 4	Run 5	Run 6	Run 7	Run 8	Run 9	Run 10	Run 11	Run 12
c_v	4000	4000	4000	4000	4000	4000	4000	4000	4000	4000	4000	4000
σ	100	100	100	100	100	100	100	100	100	100	100	100
Δt	0.001	0.01	0.25	0.001	0.01	0.25	0.001	0.01	0.25	0.001	0.01	0.25
Δx	10	10	10	1	1	1	0.1	0.1	0.1	0.01	0.01	0.01
$1/(\sigma\Delta x)$	0.001	0.001	0.001	0.01	0.01	0.01	0.1	0.1	0.1	1	1	1
sqrt($c\Delta t/\sigma$)/Δx	3E-04	0.001	0.005	0.003	0.01	0.05	0.032	0.1	0.5	0.316	1	5
E_e/E_c	0.1	0.999	24.39	0.1	0.999	24.39	0.1	0.999	24.39	0.1	0.999	24.39
Improvement	Best	Sig.	Sig.	Sig.	Sig.	Sig.	Lim.	Sig.	Lim.	None	Lim.	None

are 10000 particles per time step, and $c_v = 4T^3$.

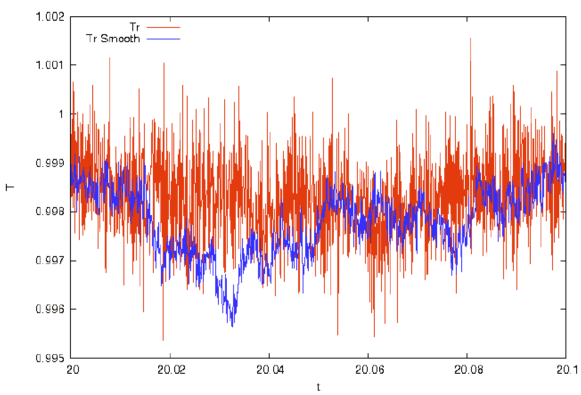

(a) Zone 1

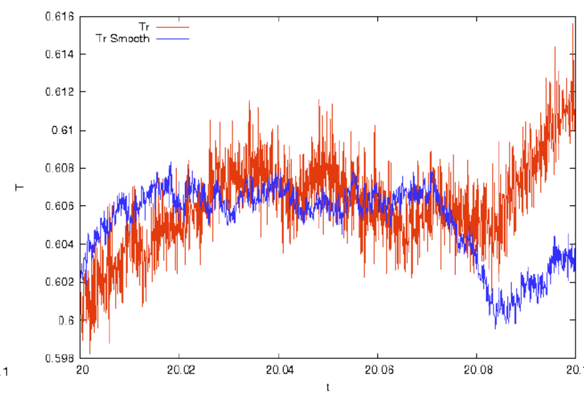

(b) Zone 5

Figure 7: Radiation temperature in a Marshak wave test problem simulated by standard IMC (T_r) and by smooth emission IMC (T_r Smooth) shown over a short time scale. $1/(\sigma\Delta x) = 0.01$, $\sqrt{c\Delta t/\sigma}/\Delta x = 0.05475$, and $E_{emitted}/E_{census} = 21.24$.

Figures 7 and 8 show the radiation temperature versus time in the boundary zone and an interior zone. For this problem, $1/(\sigma\Delta x) = 0.01$, $\sqrt{c\Delta t/\sigma}/\Delta x = 0.05475$, and $E_{emitted}/E_{census} = 21.24$, and so the smooth emission algorithm should reduce the noise. In Fig. 7, which shows the results over a short time scale, we see that the smooth emission result is generally less noisy. However, we see that the solution can still drift significantly over the course of many time steps as particles cross zone boundaries. As a result, over long time scales, the two methods are in close agreement, but both show similarly large drifts, and it is difficult to know which is more accurate at any given point in time (Fig. 8).

Finally, we will study the effectiveness of the smooth emission algorithm in simulating a radiating shock. The test problem is one developed by Lowrie and Edwards and has a known semi-

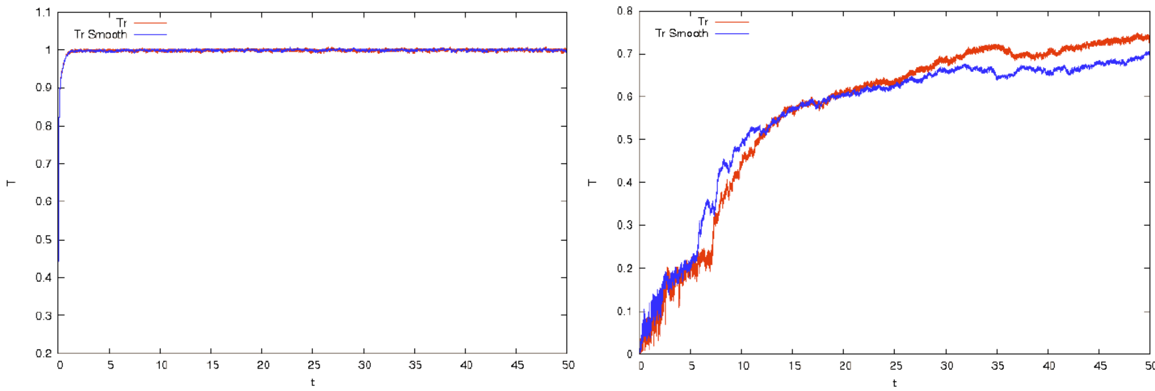

(a) Zone 1 (b) Zone 5

Figure 8: Radiation temperature in a Marshak wave test problem simulated by standard IMC (T_r) and by smooth emission IMC (T_r Smooth) shown over a long time scale. $1/(\sigma\Delta x) = 0.01$, $\sqrt{c\Delta t/\sigma}/\Delta x = 0.05475$, and $E_{emitted}/E_{census} = 21.24$.

analytic solution (Lowrie and Edwards, 2007). It is a mach 45 shock traveling through an opaque medium. The matter is an ideal gas with $\gamma = 5/3$ and $c_v = 1.447 \times 10^{15}$ erg/(g-keV). It is a purely absorbing medium with $\sigma_a = \sigma_0 \rho^2 T^{-3.5}$, and $\sigma_0 = 85.27$ cm^5 keV$^{3.5}$ / g^2. Ahead of the shock, $\rho = 1.0$ g/cm^3, $v = 0$ cm/s, and $T_m = T_r = 0.1$ keV. Behind the shock, $\rho = 6.426$ g/cm^3, $v = -4.818 \times 10^8$ cm/s, and $T_m = T_r = 8.36$ keV. The velocity of the shock is $v_{shock} = -5.71 \times 10^8$ cm/s. The mesh contains 5000 zones that are initially of equal size and spanning $x \in [0, 2500]$ cm. There are 10^6 photons per time step. Ahead of the shock, $1/(\sigma\Delta x) = 7.417 \times 10^{-6}$, $\sqrt{c\Delta t/\sigma}/\Delta x = 0.006669$, and $E_{emitted}/E_{census} = 2628$, while behind the shock, $1/(\sigma\Delta x) = 0.9587$, $\sqrt{c\Delta t/\sigma}/\Delta x = 2.397$, and $E_{emitted}/E_{census} = 0.02888$. Therefore, we would expect the smooth emission algorithm to reduce noise ahead of the shock, but not behind it.

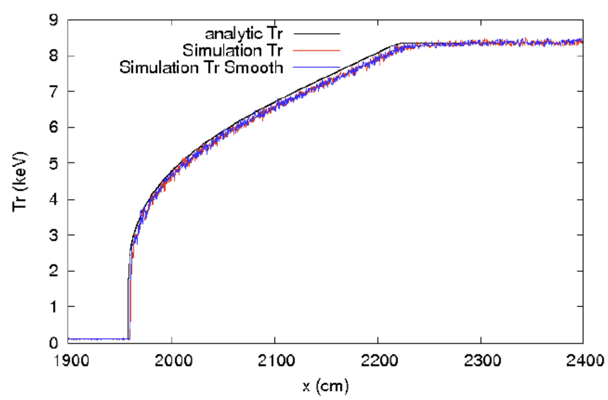

Figure 9: Radiation temperature for a Mach 45 shock at $t = 14.0219 \times 10^{-8}$ s from a standard IMC simulation (Simulation T_r), from a smooth emission IMC simulation (Simulation T_r Smooth), and from an analytic solution (analytic T_r).

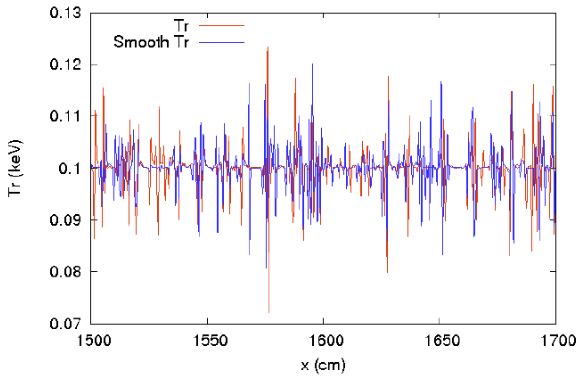

(a) Ahead of the Shock Front

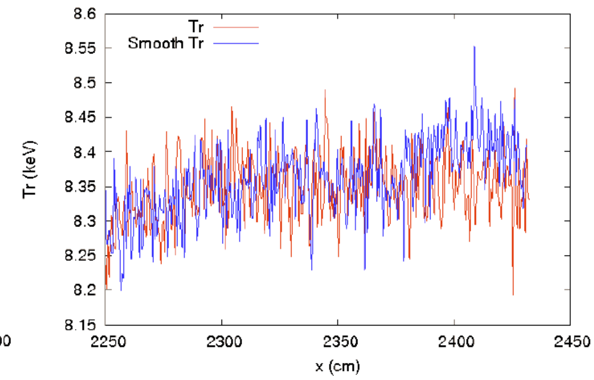

(b) Behind the Shock Front

Figure 10: Radiation temperature for a Mach 45 shock at $t = 14.0219 \times 10^{-8}$ s from a standard IMC simulation (T_r) and from a smooth emission IMC simulation (T_r Smooth) ahead of and behind the shock.

In Fig. 9, we see that smooth emission IMC and standard IMC both agree well with the analytic solution. Figure 10 shows the radiation temperature as a funcntion of space ahead of and behind the shock after many time steps. As we have shown, over long time scales the solution can drift substantially, and as a result, the spatial solution is still noisy this far into the simulation.

5. Conclusions

In this paper, we have demonstrated that the random sampling of source photon emission times can be eliminated from the IMC algorithm. Instead, we consider energy contributions from all possible emission times and analytically calculate the average.

This new treatment of photon sources eliminates noise in one zone, grey, infinite medium problems. The new algorithm reduces noise in multizone problems in which most source photons remain in the zone they were emitted in. It is more effective in problems in which the number of source photons is large compared to the number of census photons.

However, the zone temperatures can still exhibit large jumps when particles cross zone boundaries. As a result, over long time scales the new algorithm has little effect on the solution.

In the future, we intend to implement a stratified sampling algorithm for the position and angle of source photons. Stratified sampling should reduce noise arising from the random sampling of the spatial and angular variables. When combined with analytic treatment of photon emission time, stratified sampling of the position and angle of emitted photons may reduce noise in IMC calculations.

Acknowledgments

The work of the first author was supported by the DOE Computational Science Graduate Fellowship, Grant Number DE-FG02-97ER25308. The work of the second author was performed under the auspices of the U.S. Department of Energy by Lawrence Livermore National Laboratory under Contract DE-AC52-07NA27344.

REFERENCES

1. Pomraning, G.C. (2005). *The Equations of Radiation Hydrodynamics.* Dover Publications, Mineola, NY.

2. Fleck, J.A. Jr., Cummings, J.A. (1971). An Implicit Monte Carlo Scheme for Calculating Time and Frequency Dependent Nonlinear Radiation Transport. *J. Comput. Phys.*, **8**: 313-342.

3. Gentile, N.A., Trahan, T.J. (2011). A Modified Treatment of Sources in Implicit Monte Carlo Radiation Transport. *22nd International Conference on Transport Theory*, Portland, OR.

4. Kalos, M.A., Whitlock, P.A. (2008). *Monte Carlo Methods, Second Edition.* Wiley-VCH, Weinheim, Germany.

5. Lowrie, R.B., Edwards, J.D. (2007). Shock Wave Solutions for Radiation Hydrodynamics. *Joint International Topical Meeting on Mathematics & Computation and Supercomputing in Nuclear Applications (M&C + SNA 2007)*, Monterey, CA.

6. Lowrie, R.B., Edwards, J.D. (2007). Radiative Shock Solutions with Gray Nonequilibrium Diffusion. *Shock Waves*, **18**: 129-143.